

Cosmic ray mass composition measurement with the TALE hybrid detector

Keitaro Fujita^{a,*} for the Telescope Array collaboration

*^aInstitute for Cosmic Ray Research, the University of Tokyo,
5-1-5 Kashiwa-no-Ha, Kashiwa, Chiba, Japan*

E-mail: kfujita@icrr.u-tokyo.ac.jp

We report on the cosmic ray mass composition measured by the Telescope Array Low-energy Extension (TALE) hybrid detector. The TALE detector consists of a Fluorescence Detector (FD) station with 10 FD telescopes located at the TA Middle Drum FD Station (itself made up of 14 FD telescopes), and a Surface Detector (SD) array of scintillation counters. The SD array consists of 40 counters with 400 m spacing and 40 counters with 600 m spacing. The FD station, with a total of 24 telescopes, overlooks the SD array and provides sky coverage with an elevation angle range of 3° to 59°. In this contribution, we will present the latest result of the cosmic ray mass composition measurement in the energy range from $10^{16.5}$ eV to $10^{18.5}$ eV using almost 5 years of TALE hybrid data.

The 38th International Cosmic Ray Conference (ICRC2023)
26 July – 3 August, 2023
Nagoya, Japan



*Speaker

1. Introduction

The Telescope Array located around 39° S, 113° W has the largest cosmic ray observatory in the northern hemisphere, designed to detect ultra high energy cosmic rays. The main part of the experiment consists of a SD array and three FD stations that overlook the SD area. The TA SD deployed 507 scintillation counters in a square grid with 1200 m spacing, covering a total of ~ 700 km² area on the ground. Each surface counter has two layers of a plastic scintillators each with an area of 3 m² and a thickness of 1.2 cm. The scintillation light produced by the charged particles energy deposition are guided to the photomultipliers that connected from each layer through wavelength shifting fibers [1]. The three TA FD stations are located at Black Rock Mesa (BRM), Long Ridge (LR), and Middle Drum (MD). The stations have a viewing range of 3° to 31° in elevation. A fluorescence telescope of TA is composed of a segmented spherical mirror and a camera of 256 hexagonal photomultipliers, with a field of view is $1^\circ \times 1^\circ$ [2].

In addition to the main TA experiment, the Telescope Array Low-energy Extension (TALE), located at the north part of the site, is aimed at measuring the very high energy cosmic rays above 10^{16} eV to reveal the nature of the transition from galactic to extra-galactic cosmic rays. The TALE detector consists of one FD station with ten fluorescence telescopes and an array of 80 scintillation surface detectors, which were deployed to cover a total area of approximately 20 km². The TALE FD began operation in 2013 at the MD station. The ten fluorescence telescopes used in TALE were refurbished from components previously employed by the HiRes experiment [3]. These telescopes have a field of view ranging from 31° to 59° in elevation, directly above the field of view of the MD telescopes. The TALE SD consists of 40 scintillation counters with 400 m and 40 counters with 600 m spacing, and started observation from 2017. In addition, an external trigger from the TALE FD to the TALE SD to detect low energy cosmic ray showers, so-called hybrid trigger system, was installed in 2018. The TALE detector configuration is shown in Fig. 1. The full details of the detectors are found in [4–6]. We will present the latest result of the cosmic ray mass composition measurement using almost 5 years of the TALE hybrid observation data including the MD telescope data, for which the deeper X_{\max} showers can be detected by the lower field of view. The combination of sky coverage by MD and TALE FD provides more uniform X_{\max} acceptance for interest energy range.

2. Event Reconstruction

In the energy range of just below 10^{17} eV, we use the TALE FD as an Imaging Air Cerenkov Telescope (IACT) to extend the energy threshold of the detector down to $\sim 10^{15}$ eV. The Cherenkov light produced by a shower has the same characteristic as fluorescence light, being directly proportional to the number of shower particles for any given point in the shower development. This property means that the observed Cherenkov signal can be used to infer the shower properties (energy and X_{\max}) in a similar way to how the fluorescence light is used. A significant difference between Cherenkov light and fluorescence light is that the Cherenkov light emitted by the shower particles is strongly peaked forward along the shower direction, and falls off rapidly as the shower viewing angle changes while the fluorescence light is emitted isotropically. As a result, Cherenkov events are seen only if the shower geometry with respect to the detector is such that the shower

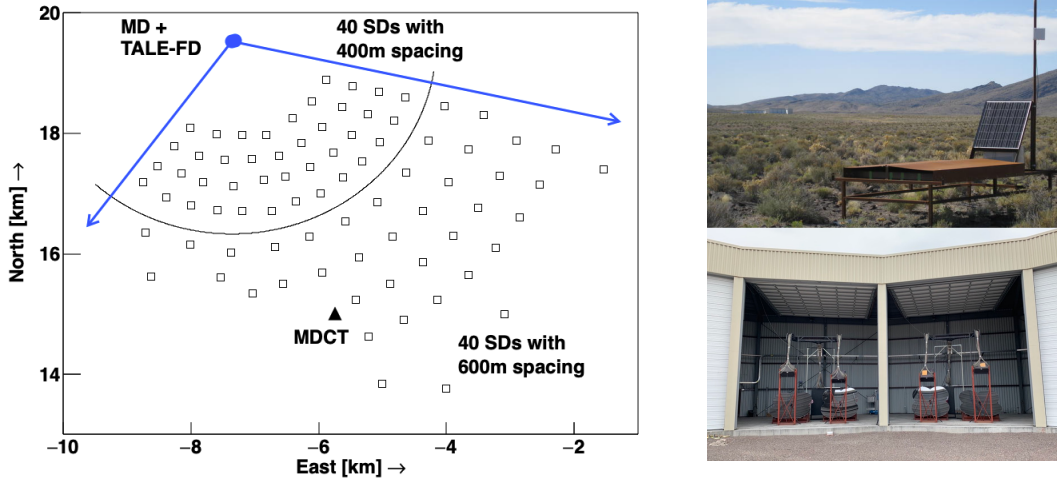


Figure 1: Left: The layout of the TALE detector. Open square boxes represent the locations of the TALE SD counters and a small filled circle corresponds to the MD / TALE FD station. The arrows represent azimuthal viewing ranges of both FDs. Top-Right: A deployed SD in the field. Bottom-Right: The photograph of TALE telescopes in the FD station.

is moving towards the detector (viewing angle $\sim 10^\circ$ or smaller), and are observed much faster (total event duration and shower image are much shorter) than fluorescence dominated events seen by main TA hybrid detector where energies above 10^{18} eV. Due to the above reasons, the lower energy events seen by Cherenkov light are processed for reconstruction by the Profile-Constrained Geometry Fit (PCGF) that simultaneously reconstructs the shower geometry and the shower profile, originally developed by the HiRes collaboration [7]. This method scans over all possible shower geometries compatible with the arrival times of photons at individual pixels of the FD camera and for each such geometry calculates a trial shower profile in the atmosphere. In this work, the possible shower geometries are provided by a process of the hybrid geometry calculation that combines the timing information from the FD and SD to constrain the arrival time and impact point of the shower at the ground. The shower profile fitting in given shower geometry uses the Gaisser-Hillas parameterization formula [8]

$$N(x) = N_{\max} \left(\frac{x - X_0}{X_{\max} - X_0} \right)^{\frac{X_{\max} - X_0}{\lambda}} \exp \left(-\frac{X_{\max} - x}{\lambda} \right), \quad (1)$$

where $N(x)$ is the number of charged particles at a given slant depth, x , X_{\max} is the depth of shower maximum, N_{\max} is the maximum number of particles at X_{\max} , X_0 is the depth of the first interaction, and λ is the interaction length of shower particles. The best expectation of the shower geometry and longitudinal profile is chosen.

3. Monte Carlo Simulation and Data / MC Comparison

We run the Monte Carlo simulations to evaluate our detector performance and reconstruction resolution. In this work we generated three primary cosmic rays particles; proton, nitrogen, and

iron based on the QGSJetII-04 [9] hadronic interaction model. Equal numbers of events were generated for each primary type. The generated MC follows a broken power law spectrum in which the spectrum index is -2.9 below $10^{17.1}$ eV and is -3.2 above $10^{17.1}$ eV, where each parameter comes from observable values by the TALE FD monocular spectrum measurement [5]. All of the calibration factors with time dependence are considered in the SD and FD detector simulations. All reconstructed events are subjected to the quality cuts summarized in Table 1. The criteria were divided into two parts by the contribution of the flux of fluorescence and Cherenkov light from the air shower due to different characteristics of the fluorescence/Cherenkov dominated events. The obtained shower parameter resolutions energies above $10^{16.5}$ eV are 30 g/cm^2 in X_{max} and 10% in energy (Fig. 2). In addition, Data/MC comparisons were performed to verify that the observed events are well reproduced by our MC simulations, as shown in Fig. 3. The same quality cuts were applied to the data and the MC events.

Variable	CL	FL
No saturated PMTs in FD		applied
X_{max} bracketing cut		applied
Angular track-length [deg]	$> 6.5^\circ$	-
Event duration [ns]	$> 100 \text{ ns}$	-
# of PMTs	> 10	-
# of Photo-electrons	> 1000	> 2000

Table 1: we define events of which fractional contribution of Fluorescence Light (FL) to the total signal exceeds 0.75 as fluorescence events, and events of which fractional contribution of FL to the total signal less than or equal to 0.75 as Cherenkov Light (CL) events.

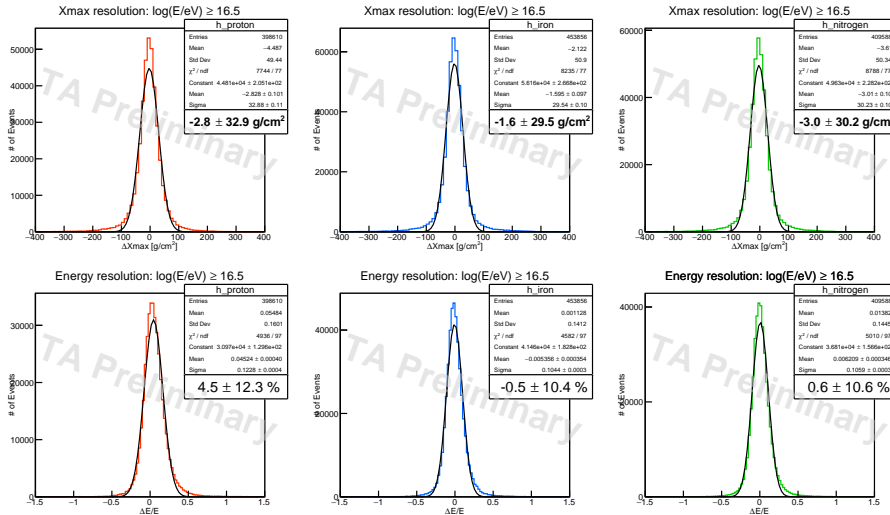


Figure 2: Reconstruction resolutions of the shower maximum X_{max} , and the shower energy E , respectively. The X_{max} resolutions for each primary are shown in the top panels, and the energy resolutions are in the bottom panels.

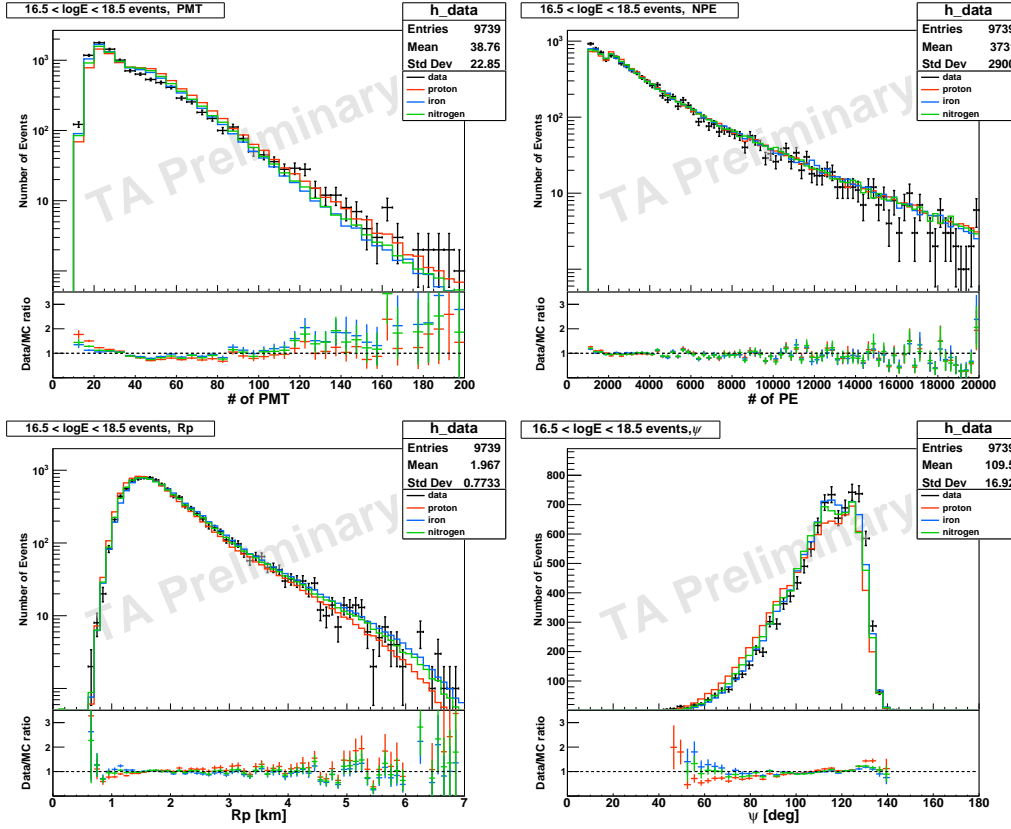


Figure 3: Data / MC comparisons. From top left to right bottom, the number of PMTs, the number of photo-electrons, the impact parameter R_p , the shower inclination angle in the shower detector plane, ψ are shown, respectively. The black points with error bars show the data, while the proton/nitrogen/iron MC are shown by the red/green/blue histograms. The MC distributions have been normalized to the same number of entries as the data.

4. Data Analysis

We present the preliminary results of the cosmic rays mass composition in the energy range from $10^{16.5}$ eV to $10^{18.5}$ eV measured with the TALE hybrid data. The result for the mean of the shower maximum, $\langle X_{\max} \rangle$, and the width of the observed X_{\max} distributions, $\sigma(X_{\max})$, as a function of the shower energy are presented in Fig. 4. For the comparison, the pure proton, pure nitrogen, and pure iron predictions calculated by our Monte-Carlo simulation are also shown beside the observed ones. In the left panel of Fig. 4, the observed elongation rate shows clearly a break, where the energy is just above 10^{17} eV. The elongation rate before the break energy is 23 ± 5 g/cm²/decade and after the break energy is 98 ± 5 g/cm²/decade, while the pure composition assumptions are around 60 g/cm²/decade, respectively. On the other hand, the $\sigma(X_{\max})$ is compatible with or wider than pure proton assumption in whole energies.

We also estimate the primary fraction of cosmic rays using TFractionFitter [10, 11]. Data X_{\max} distributions were divided into each energy bin with a width of 0.1 in $\log_{10}(E/\text{eV})$ below $10^{17.9}$

eV, for 0.2 in $\log_{10}(E/eV)$ up to $10^{18.5}$ eV. These distributions were fitted using those of MC ones containing three primaries. Fit results are shown in Fig. 5. The nitrogen fraction becomes dominant at $10^{16.7}$ eV, then iron fraction follows at higher energies as expected by the Peters cycle [12] while the low contribution of proton primary at around 10^{17} eV.

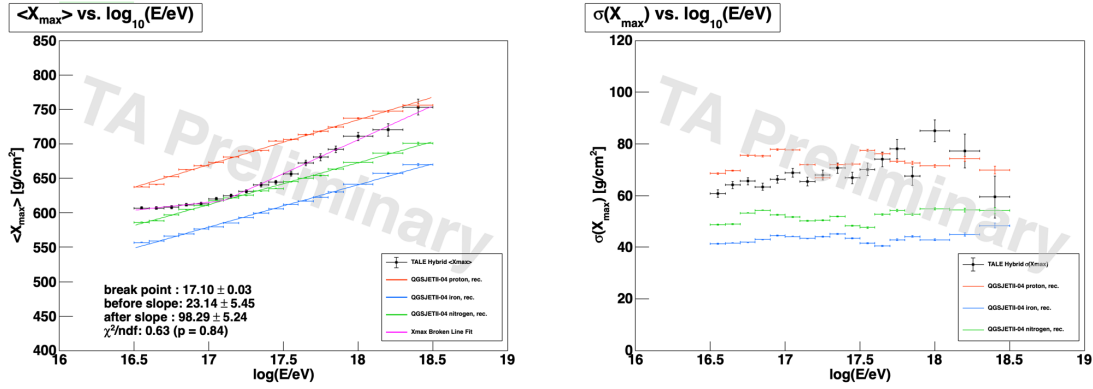


Figure 4: Top: $\langle X_{\max} \rangle$ as a function of shower energy, measured by using 5 years of the TALE hybrid data. Bottom: $\sigma(X_{\max})$ as a function of shower energy. For both panel, the proton, nitrogen, and iron MC rails are also shown for comparison.

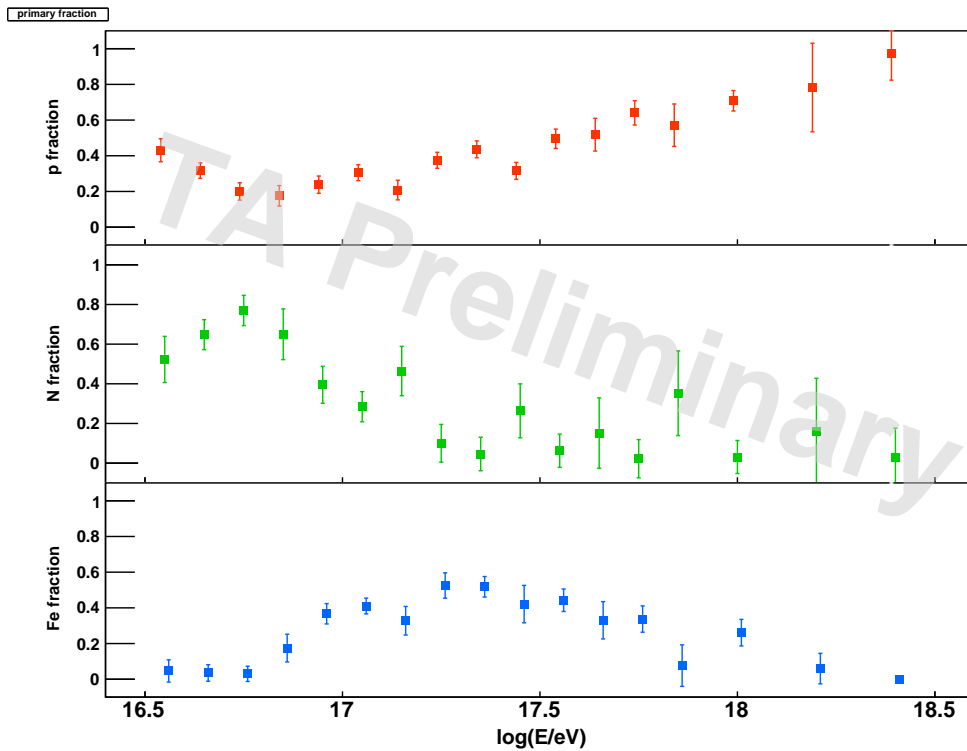


Figure 5: Primary cosmic ray fraction estimated by fitting of MC distributions with the hadronic interaction model of QGSJetII-04. From top to bottom, estimated proton fraction, nitrogen, and iron one are displayed.

5. Conclusion

We reported on the preliminary result of the mass composition measurement obtained by using 5 years of TALE hybrid data. In this contribution, we presented the measured $\langle X_{\max} \rangle$ and $\sigma(X_{\max})$ as a function of primary energy. The $\langle X_{\max} \rangle$ elongation rate shows a change in the slope at the energy just above 10^{17} eV. This break in the elongation rate is likely correlated with the observed break in the cosmic ray energy spectrum by the TALE FD monocular measurement [5]. Furthermore, we estimate the primary cosmic rays fraction by fitting the data X_{\max} distributions to the MC ones. These results are consistent with a picture that the transition of the origin of the galactic cosmic rays to the extra-galactic cosmic rays is around "2nd knee", at around 10^{17} eV, with which the changing of the elongation rate in the mean X_{\max} while a wider X_{\max} distribution at these energies due to the mixed composition of heavier galactic cosmic rays and lighter component of extra-galactic one.

Acknowledgements

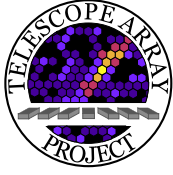
The Telescope Array experiment is supported by the Japan Society for the Promotion of Science(JSPS) through Grants-in-Aid for Priority Area 431, for Specially Promoted Research JP21000002, for Scientific Research (S) JP19104006, for Specially Promoted Research JP15H05693, for Scientific Research (S) JP19H05607, for Scientific Research (S) JP15H05741, for Science Research (A) JP18H03705, for Young Scientists (A) JPH26707011, and for Fostering Joint International Research (B) JP19KK0074, by the joint research program of the Institute for Cosmic Ray Research (ICRR), The University of Tokyo; by the Pioneering Program of RIKEN for the Evolution of Matter in the Universe (r-EMU); by the U.S. National Science Foundation awards PHY-1806797, PHY-2012934, PHY-2112904, PHY-2209583, and PHY-2209584 as well as AGS-1613260, AGS-1844306, and AGS-2112709; by the National Research Foundation of Korea (2017K1A4A3015188, 2020R1A2C1008230, & 2020R1A2C2102800) ; by the Ministry of Science and Higher Education of the Russian Federation under the contract 075-15-2020-778, IISN project No. 4.4501.18, by the Belgian Science Policy under IUAP VII/37 (ULB), by National Science Centre in Poland grant 2020/37/B/ST9/01821. This work was partially supported by the grants of the joint research program of the Institute for Space-Earth Environmental Research, Nagoya University and Inter-University Research Program of the Institute for Cosmic Ray Research of University of Tokyo. The foundations of Dr. Ezekiel R. and Edna Wattis Dumke, Willard L. Eccles, and George S. and Dolores Doré Eccles all helped with generous donations. The State of Utah supported the project through its Economic Development Board, and the University of Utah through the Office of the Vice President for Research. The experimental site became available through the cooperation of the Utah School and Institutional Trust Lands Administration (SITLA), U.S. Bureau of Land Management (BLM), and the U.S. Air Force. We appreciate the assistance of the State of Utah and Fillmore offices of the BLM in crafting the Plan of Development for the site. We thank Patrick A. Shea who assisted the collaboration with much valuable advice and provided support for the collaboration's efforts. The people and the officials of Millard County, Utah have been a source of steadfast and warm support for our work which we greatly appreciate. We are indebted to the Millard County Road Department for their efforts to maintain and clear the roads which get us to our sites. We gratefully acknowledge the contribution from the technical staffs of our home institutions. An allocation of

computing resources from the Center for High Performance Computing at the University of Utah as well as the Academia Sinica Grid Computing Center (ASGC) is gratefully acknowledged.

References

- [1] **Telescope Array** collaboration, T. Abu-Zayyad, R. Aida, M. Allen, R. Anderson, R. Azuma, E. Barcikowski et al., *Nucl. Instrum. Meth. A* **689** (2012) 87.
- [2] **Telescope Array** collaboration, H. Tokuno et al., *Nucl. Instrum. Meth. A* **676** (2012) 54 [1201.0002].
- [3] J.H. Boyer, B.C. Knapp, E.J. Mannel and M. Seman, *Nucl. Instrum. Meth. A* **482** (2002) 457.
- [4] **Telescope Array** collaboration, S. Ogio, *PoS ICRC2019* (2019) 375.
- [5] **Telescope Array** collaboration, R.U. Abbasi et al., *Astrophys. J.* **865** (2018) 74 [1803.01288].
- [6] **Telescope Array** collaboration, R.U. Abbasi et al., *Nucl. Instrum. Meth. A* **1019** (2021) 165726 [2103.01086].
- [7] **HiRes** collaboration, R.U. Abbasi et al., *Phys. Rev. Lett.* **100** (2008) 101101 [astro-ph/0703099].
- [8] T.K.Gaisser and A.M.Hillas, vol. Proceedings of 15th International Cosmic Ray Conference (Plovdiv, Bulgaria) 8, 1977.
- [9] S. Ostapchenko, *Phys. Rev. D* **83** (2011) 014018 [1010.1869].
- [10] TFractionFitter. <https://root.cern/doc/master/classTFractionFitter.html>.
- [11] R.J. Barlow and C. Beeston, *Comput. Phys. Commun.* **77** (1993) 219.
- [12] B. Peters, *Il Nuovo Cimento (1955-1965)* **22** (1961) 800.

Full Authors List: The Telescope Array Collaboration



R.U. Abbasi¹, Y. Abe², T. Abu-Zayyad^{1,3}, M. Allen³, Y. Arai⁴, R. Arimura⁴, E. Barcikowski³, J.W. Belz³, D.R. Bergman³, S.A. Blake³, I. Buckland³, B.G. Cheon⁵, M. Chikawa⁶, A. Fedynitch^{6,7}, T. Fujii^{4,8}, K. Fujisue⁶, K. Fujita⁶, R. Fujiwara⁴, M. Fukushima⁶, G. Furlich³, Z. Gerber³, N. Globus^{9*}, W. Hanlon³, N. Hayashida¹⁰, H. He⁹, R. Hibi², K. Hibino¹⁰, R. Higuchi⁹, K. Honda¹¹, D. Ikeda¹⁰, N. Inoue¹², T. Ishii¹¹, H. Ito⁹, D. Ivanov³, A. Iwasaki⁴, H.M. Jeong¹³, S. Jeong¹³, C.C.H. Jui³, K. Kadota¹⁴, F. Kakimoto¹⁰, O. Kalashev¹⁵, K. Kasahara¹⁶, S. Kasami¹⁷, S. Kawakami⁴, K. Kawata⁶, I. Kharuk¹⁵, E. Kido⁹, H.B. Kim⁵, J.H. Kim³, J.H. Kim^{3†}, S.W. Kim¹³, Y. Kimura⁴, I. Komae⁴, K. Komori¹⁷, Y. Kusumori¹⁷, M. Kuznetsov^{15,18}, Y.J. Kwon¹⁹, K.H. Lee⁵, M.J. Lee¹³, B. Lubsandorzhiiev¹⁵, J.P. Lundquist^{3,20}, T. Matsuyama⁴, J.A. Matthews³, J.N. Matthews³, R. Mayta⁴, K. Miyashita², K. Mizuno², M. Mori¹⁷, M. Murakami¹⁷, I. Myers³, S. Nagataki⁹, K. Nakai⁴, T. Nakamura²¹, E. Nishio¹⁷, T. Nonaka⁶, S. Ogio⁶, H. Ohoka⁶, N. Okazaki⁶, Y. Oku¹⁷, T. Okuda²², Y. Omura⁴, M. Onishi⁶, M. Ono⁹, A. Oshima²³, H. Oshima⁶, S. Ozawa²⁴, I.H. Park¹³, K.Y. Park⁵, M. Potts^{3‡}, M.S. Pshirkov^{15,25}, J. Remington³, D.C. Rodriguez³, C. Rott^{3,13}, G.I. Rubtsov¹⁵, D. Ryu²⁶, H. Sagawa⁶, R. Saito², N. Sakaki⁶, T. Sako⁶, N. Sakurai⁴, D. Sato², K. Sato⁴, S. Sato¹⁷, K. Sekino⁶, P.D. Shah³, N. Shibata¹⁷, T. Shibata⁶, J. Shikita⁴, H. Shimodaira⁶, B.K. Shin²⁶, H.S. Shin⁶, D. Shinto¹⁷, J.D. Smith³, P. Sokolsky³, B.T. Stokes³, T.A. Stroman³, Y. Takagi¹⁷, K. Takahashi⁶, M. Takamura²⁷, M. Takeda⁶, R. Takeishi⁶, A. Taketa²⁸, M. Takita⁶, Y. Tameda¹⁷, K. Tanaka²⁹, M. Tanaka³⁰, S.B. Thomas³, G.B. Thomson³, P. Tinyakov^{15,18}, I. Tkachev¹⁵, H. Tokuno³¹, T. Tomida², S. Troitsky¹⁵, R. Tsuda⁴, Y. Tsunesada^{4,8}, S. Udo¹⁰, F. Urban³², I.A. Vaiman¹⁵, D. Warren⁹, T. Wong³, K. Yamazaki²³, K. Yashiro²⁷, F. Yoshida¹⁷, Y. Zhezher^{6,15}, and Z. Zundel³

¹ Department of Physics, Loyola University Chicago, Chicago, Illinois 60660, USA

² Academic Assembly School of Science and Technology Institute of Engineering, Shinshu University, Nagano, Nagano 380-8554, Japan

³ High Energy Astrophysics Institute and Department of Physics and Astronomy, University of Utah, Salt Lake City, Utah 84112-0830, USA

⁴ Graduate School of Science, Osaka Metropolitan University, Sugimoto, Sumiyoshi, Osaka 558-8585, Japan

⁵ Department of Physics and The Research Institute of Natural Science, Hanyang University, Seongdong-gu, Seoul 426-791, Korea

⁶ Institute for Cosmic Ray Research, University of Tokyo, Kashiwa, Chiba 277-8582, Japan

⁷ Institute of Physics, Academia Sinica, Taipei City 115201, Taiwan

⁸ Nambu Yoichiro Institute of Theoretical and Experimental Physics, Osaka Metropolitan University, Sugimoto, Sumiyoshi, Osaka 558-8585, Japan

⁹ Astrophysical Big Bang Laboratory, RIKEN, Wako, Saitama 351-0198, Japan

¹⁰ Faculty of Engineering, Kanagawa University, Yokohama, Kanagawa 221-8686, Japan

¹¹ Interdisciplinary Graduate School of Medicine and Engineering, University of Yamanashi, Kofu, Yamanashi 400-8511, Japan

¹² The Graduate School of Science and Engineering, Saitama University, Saitama, Saitama 338-8570, Japan

¹³ Department of Physics, SungKyunKwan University, Jang-an-gu, Suwon 16419, Korea

¹⁴ Department of Physics, Tokyo City University, Setagaya-ku, Tokyo 158-8557, Japan

¹⁵ Institute for Nuclear Research of the Russian Academy of Sciences, Moscow 117312, Russia

¹⁶ Faculty of Systems Engineering and Science, Shibaura Institute of Technology, Minato-ku, Tokyo 337-8570, Japan

¹⁷ Graduate School of Engineering, Osaka Electro-Communication University, Neyagawa-shi, Osaka 572-8530, Japan

¹⁸ Service de Physique Théorique, Université Libre de Bruxelles, Brussels, Belgium

¹⁹ Department of Physics, Yonsei University, Seodaemun-gu, Seoul 120-749, Korea

²⁰ Center for Astrophysics and Cosmology, University of Nova Gorica, Nova Gorica 5297, Slovenia

²¹ Faculty of Science, Kochi University, Kochi, Kochi 780-8520, Japan

²² Department of Physical Sciences, Ritsumeikan University, Kusatsu, Shiga 525-8577, Japan

²³ College of Science and Engineering, Chubu University, Kasugai, Aichi 487-8501, Japan

²⁴ Quantum ICT Advanced Development Center, National Institute for Information and Communications Technology, Koganei, Tokyo 184-8795, Japan

²⁵ Sternberg Astronomical Institute, Moscow M.V. Lomonosov State University, Moscow 119991, Russia

²⁶ Department of Physics, School of Natural Sciences, Ulsan National Institute of Science and Technology, UNIST-gil, Ulsan 689-798, Korea

²⁷ Department of Physics, Tokyo University of Science, Noda, Chiba 162-8601, Japan

²⁸ Earthquake Research Institute, University of Tokyo, Bunkyo-ku, Tokyo 277-8582, Japan

²⁹ Graduate School of Information Sciences, Hiroshima City University, Hiroshima, Hiroshima 731-3194, Japan

³⁰ Institute of Particle and Nuclear Studies, KEK, Tsukuba, Ibaraki 305-0801, Japan

³¹ Graduate School of Science and Engineering, Tokyo Institute of Technology, Meguro, Tokyo 152-8550, Japan

³² CEICO, Institute of Physics, Czech Academy of Sciences, Prague 182 21, Czech Republic

* Presently at: University of California - Santa Cruz

† Presently at: Argonne National Laboratory, Physics Division, Lemont, Illinois 60439, USA

‡ Presently at: Georgia Institute of Technology, Physics Department, Atlanta, Georgia 30332, USA